Journal of Membrane Science 700 (2024) 122659

Contents lists available at ScienceDirect

Journal of Membrane Science

journal homepage: www.elsevier.com/locate/memsci

Modelling of selective ion partitioning between ion-exchange membranes and highly concentrated multi-ionic brines

Giorgio Purpura [a], Ewa Papiewska [b], Andrea Culcasi [a], Antonia Filingeri [a], Alessandro Tamburini [a,*], Maria Chiara Ferrari [b], Giorgio Micale [a], Andrea Cipollina [a]

[a] Dipartimento di Ingegneria, Università Degli Studi di Palermo (UNIPA), Viale Delle Scienze, Ed 6, 90128, Palermo, Italy
[b] Chemical Engineering Department, The University of Edinburgh, Robert Stevenson Road, The King's Buildings, Edinburgh, UK

ARTICLE INFO

Keywords:
Ion exchange membranes
Selective ion partitioning
Manning model
Counter-ions condensation
Multi-ionic solutions

ABSTRACT

In recent years, the growing interest in the use of Ion-Exchange Membranes, in the treatment of highly concentrated multi-ionic brines for the selective recovery of critical elements, has prompted the research of fundamental models capable of predicting the IEMs selectivity towards like-charged species. Prior studies have proposed ion partitioning models limited to single-salt solutions that were validated only up to moderate salt concentrations. In this work, we developed a novel multi-ionic extension of the Manning counter-ion condensation model, aiming to predict the sorption selectivity of like-charged counter-ions. Furthermore, the peNRTL model was coupled with the extended Manning model to broaden its applicability range, encompassing membrane equilibrated with very highly concentrated solutions. Novel experimental ion sorption tests with single-salt and binary solutions including NaCl, KCl, $MgCl_2$, and $CaCl_2$ at high concentrations were performed with the commercial cation-exchange membrane Fumasep FKE-50. To the best of Authors' knowledge, the proposed model for the first time successfully provided quantitative predictions of multi-ionic ion partitioning for all the systems investigated up to extremely high external salt concentrations. The outcomes of this work suggest a strong influence of the local non-electrostatic interactions on the activity coefficients in the membrane phase at high external concentration and highlight the key role of counter-ions hydration state in the condensation phenomenon.

1. Introduction

Ion-Exchange Membranes (IEMs) are an important class of dense polymeric membranes made of cross-linked polymers bearing ionizable functional groups. Depending on the sign of the fixed charges, IEMs are classified as Cation-Exchange Membranes (CEMs), which bear negatively charged fixed groups, and Anion-Exchange Membranes (AEMs), which carry positively charged fixed groups. IEMs are widely adopted in various fields, including water desalination, energy storage and conversion, and chemical production. Electromembrane technologies such as ElectroDialysis (ED) [1], ElectroDialysis with Bipolar Membranes (EDBM) [2], and Capacitive De-ionization (CDI) [3] employ IEMs to separate different ionic species through their ability to act as selective mass-transport barriers. When an IEM is equilibrated with an electrolytic solution, the presence of ionised groups within the polymeric matrix causes an electrostatic potential difference at the solution-membrane interface, commonly referred to as the Donnan potential. This potential difference hinders the sorption of like-charged ions (i.e., co-ions) and promotes the sorption of oppositely charged ions (i.e., counter-ions) [4]. This mechanism, called the Donnan exclusion effect, is heavily influenced by the concentration and composition of the external solution and by the concentration of fixed charged groups (typically quantified in terms of Ion-Exchange Capacity [IEC]). For instance, the presence of multivalent counter-ions significantly weakens the Donnan exclusion effect, resulting in higher co-ion sorption and, consequently, a reduction in IEM performance in terms of neutral salt rejection [5]. In general, the performance of the electromembrane separation processes depends on the transport properties of the IEMs, such as the ionic diffusivities and the ionic conductivity. As a matter of fact, these properties are related to the equilibrium concentration of the ions in the membrane phase, which in turn depends on the external solution composition [6,7]. Understanding how ion sorption equilibria are affected by the system composition and the structural properties of the IEMs would help to guide the development of new tailor-made

* Corresponding author.
E-mail address: alessandro.tamburini@unipa.it (A. Tamburini).

https://doi.org/10.1016/j.memsci.2024.122659
Received 11 January 2024; Received in revised form 23 February 2024; Accepted 10 March 2024
Available online 13 March 2024

membranes for ion-selective separation processes, leveraging the species selectivity of the IEMs. However, despite the extensive literature on IEMs characterization and modelling, a fundamental understanding of ion partitioning is still missing [8]. This lack of fundamental knowledge is even more significant when dealing with multi-ionic solutions, as most research to date has focused on IEMs equilibrated with simple single-salt solutions. Recently, interest in the characterization and modelling of IEMs equilibrated with complex multi-ionic solutions has grown due to the development of new applications of electromembrane processes for the selective recovery of raw materials from waste brines [9,10]. Traditionally, ion sorption in charged polymers has been described using the ideal Donnan model that roughly assumes the activity coefficients in both the external solution and membrane phase to be unitary, neglecting any possible non-ideal effect [11]. In recent years, the Donnan-Manning model, derived from Manning's counter-ion condensation theory [12], has been suggested as an improved framework for predicting ion sorption in IEMs [13–15]. When properly calibrated, the model provided quantitative ion partitioning predictions for single-salt systems in the external concentration range of 0.1–1.0 $mol\,l^{-1}$ for a wide number of IEMs, especially for highly charged membranes with a high water content. However, the model yielded poor results both at very low and very high external salt concentrations [5,16]. This poor performance is probably due to the breakdown of some model assumptions or due to non-ideal phenomena strongly dependent on the external salt concentration which are not considered. Another severe limitation of the Donnan-Manning model is its inability to predict ion partitioning in a multi-ionic system, which can be attributed to the structural limitations of the model. Specifically, in Manning's original formulation, the ions are characterized only by their valence. Analogously to the Debye-Hückel model for dilute aqueous electrolyte, the Manning model in fact only considers the electrostatic interactions between the absorbed ions and the fixed charges in the polymeric matrix. Such a model would predict equal activity coefficients for all the counter-ions with the same valence, as it neglects any other species-specific effects. However, a different sorption selectivity for different counter-ions of similar valence was experimentally observed in several kinds of membranes. For instance, Galizia et al. [15] investigated the ion sorption in a commercial membrane equilibrated with different single-salt solutions, while Chen et al. [17] investigated the ion sorption of two types of commercial CEMs equilibrated with binary salt solutions. Their studies show that at fixed ionic concentration, counter-ions with a lower hydrated radius and, thus, a higher crystal radius are preferentially absorbed into the membrane. This fact suggests that the hydration state of the ions, as well as their valence, should be related to the partition selectivity (see section 2.1). Thereafter, Wang et al. proposed an extended version of the Manning model to describe the ion partition in a system containing more than one salt [18]. However, their model requires additional parameters (i.e., the condensation selectivity, see section 2.3), which need to be properly calibrated using experimental data from binary salt solution tests. In this work we developed a novel multi-ionic version of the Manning model, proposing a counter-ion condensation selectivity rule in order to reduce the number of calibration parameters while keeping a high predictive capability. Furthermore, by combining the proposed extended Manning model with the peNRTL model (outlined by Yu et al. [19]), we effectively addressed the non-ideal phenomena that the original Manning model can not capture. This advancement refines the accuracy of the model, minimizes the use of adjustable parameters, and extends the model's applicability to a wider range of concentrations, thus representing a substantial step forward in the field. Most of the ion partitioning tests reported in the literature were carried out with single-salt solutions of moderate concentration (up to 1.0 $mol\,l^{-1}$). Hence, ion partitioning tests at high external concentrations were carried out in this work in order to collect the experimental data required to validate the model over a wider range of concentrations [0.1–5.0 $mol\,l^{-1}$]. Notably, concentrations higher than 5.0 $mol\,l^{-1}$ were not investigated in order to avoid any issue relevant to local phenomena of salt precipitation. Finally, the proposed model was compared with the ideal Donnan model and the simple extended Donnan-Manning model to highlight the inherent differences between them. The result was an overwhelming superiority of the proposed model in terms of application range and predictive capability.

2. Ion partitioning modelling

The first section of this work is devoted to the theoretical background of ion partitioning and to the development and implementation of the proposed thermodynamic models.

2.1. Theoretical background

When an IEM is in contact with an aqueous electrolytic solution, water and mobile ions are absorbed into the membrane. At equilibrium condition, the electrochemical potential of each ionic species in the two phases is usually assumed to be equal. Consequently, the ion partitioning can be modelled by applying the so-called Donnan equilibria:

$$m_i^m = m_i^s \left(\frac{\gamma_i^{(m),s}}{\gamma_i^{(m),m}}\right) exp\left(-\frac{z_i F}{RT}\Delta\varphi\right) \tag{1}$$

According to the previous equation, derived in Supporting Material, the equilibrium molal concentration in membrane m_i^m is related to the external molal concentration m_i^s through the Donnan potential $\Delta\varphi$ and the ratio between the molal-based activity coefficients $\gamma_i^{(m),s}$ and $\gamma_i^{(m),m}$ in the two phases. The superscript s and m refer to the thermodynamic phase (i.e., the solution phase and the membrane phase respectively). The equilibrium concentrations of the ions in the membrane phase are also generally related to each other by the electroneutrality condition, which states that the net charge density in the membrane phase must be null:

$$\sum_i z_i m_i^m + z_{fix} m_{fix} = 0 \tag{2}$$

where z_{fix} and m_{fix} are the valence and the molal concentration of the fixed charges, respectively. Equations (1) and (2) form a finite set of equations that can be solved iteratively to obtain, as a function of the external composition, the equilibrium concentration of the ions in the membrane, if reasonable values can be provided for the ions activity coefficients in the two phases. Starting from equation (1), it is also possible to define the partitioning coefficient of the *i-th* species, K_i, and the partition selectivity between two different species $S_{i,j}$ as follows:

$$K_i = \frac{m_i^m}{m_i^s} = \left(\frac{\gamma_i^{(m),s}}{\gamma_i^{(m),m}}\right) exp\left(-\frac{z_i F}{RT}\Delta\varphi\right) \tag{3}$$

$$S_{i,j} = \frac{K_i}{K_j} = \frac{m_i^m / m_i^s}{m_j^m / m_j^s} = \left(\frac{\gamma_i^{(m),s}\gamma_j^{(m),m}}{\gamma_i^{(m),m}\gamma_j^{(m),s}}\right) exp\left(-\frac{(z_i - z_j)F}{RT}\Delta\varphi\right) \tag{4}$$

Differently from the well-known permselectivity, which is a hybrid quantity that depends on both thermodynamic and transport properties, the useful quantities previously introduced are frequently adopted to compare the thermodynamic affinity of different ionic species toward the membrane phase, thus allowing to decouple thermodynamic and transport selectivity. For instance, if $S_{i,j} > 1$ it means that the species i will be preferentially absorbed inside the membrane and vice versa if $S_{i,j} < 1$.

2.2. Ideal Donnan model

The activity coefficients in the external solution $\gamma_i^{(m),s}$ can be easily evaluated as a function of the solution composition using proper ther-

modynamic models [20,21]. However, due to the lack of models to describe the non-ideal behaviour of the membrane phase, the ratio between the activity coefficients in the two phases is usually assumed to be one. As a result, equation (1) is usually simplified as follows:

$$m_i^m = m_i^s \, exp\left(-\frac{z_i F}{RT}\Delta\varphi \right) \tag{5}$$

Equation (5) is known as the ideal Donnan equilibrium and, although well-established and traditionally adopted, is based on a rather rough approximation as the ratio between the activity coefficients in the two phases can significantly deviate from unity [4]. Consequently, the ideal Donnan model (namely equations (5) and (2)) may yield very poor predictions of mobile salt sorption. Advanced ion-partitioning models can overcome this approximation by employing a proper thermodynamic model to evaluate the activity coefficients of the ions in the membrane phase.

2.3. Extended Donnan - Manning model

The Donnan–Manning model was first proposed by Kamcev et al. [13] as an enhanced framework for predicting ion sorption in IEMs. The improvement stems from the evaluation of the activity coefficients in the membrane phase achieved through the application of the Manning model that was initially developed to describe the colligative properties of mixed salt-polyelectrolyte solutions [12]. In his work, Manning employed a Debye-Hückel approach to elucidate the electrostatic interactions between the mobile ions and the fixed charges in the polymer backbone, which was conceptualized as an infinite extended linear charge distribution. The main parameter of Manning's model is the reduced linear charge density ξ:

$$\xi = \frac{\lambda_b}{b} = \frac{e^2}{4\pi\varepsilon_r\varepsilon_0 k_B T b} \tag{6}$$

where λ_b is the Bjerrum length, b is the average distance between the fixed charges on the polyelectrolyte chain, e is the elementary charge, ε_0 is the vacuum dielectric constant, ε_r is the medium relative dielectric constant, k_B is Boltzmann's constant and T is the absolute temperature. ξ is a dimensionless parameter that describes to what extent the regions of strong electrostatic interaction near the fixed charges are overlapped. The primary implication of Manning's theory, also known as counter-ion condensation theory, is that when the reduced linear charge density ξ exceeds a specific critical threshold (see equation (10)), a portion of the counter-ions condenses onto the polymeric chain. This process virtually neutralizes a fraction of the fixed charges, thus reducing the effective linear charge density to a specific equilibrium value. The counter-ion condensation phenomenon, similar to the ion-pairing observed in highly concentrated aqueous solution, occurs when the absolute minima in the electrostatic potential approach the location of the fixed charges [8]. The condensed counter-ions are, thus, localized in a region close to the fixed charges and no longer participate in osmotic equilibria. Consequently, counter-ion condensation results in a reduction in the activity of mobile (i.e., non-condensed) ions. While the commonly used expression for the Manning activity coefficient applies only to single-salt systems, a comprehensive multi-ionic expression can be derived starting from the expression of the system's excess free energy, corresponding to the electrical work required to charge the polyelectrolyte chains [12,22]:

$$\gamma_i^{(m),M} = (1-\theta_i) exp\left[-\frac{\xi\left(1-\theta_{fix}\right)^2 m_{fix} z_{fix}^2 (1-\theta_i) z_i^2}{2\sum_j (1-\theta_j) m_j z_j^2} \right] \tag{7}$$

Equation (7), which is theoretically derived in Supporting Material, represents the multi-ionic extension of the classic Manning's model for single-salt solutions and can be applied to evaluate the Manning activity coefficient of each mobile species either when the system is condensing or not. In the previous equation, the sum at the denominator is extended to all the mobile (i.e., not fixed) species in the membrane phase. θ_{fix} and θ_i are respectively the condensed fractions of fixed charges and of the i-th ionic species, which are related to each other by the following charge balance:

$$\sum_i z_i \theta_i m_i^m + z_{fix}\theta_{fix} m_{fix} = 0 \tag{8}$$

In the previous equation (8), the sum is extended to all mobile species, with the understanding that the co-ions condensed fractions are always zero, as only counter-ions can condense. In order to solve equation (7) for the Manning activity coefficients, feasible values for the fixed charges and counter-ions condensed fractions must be provided. According to Manning's limiting law, the fixed charges condensed fraction can be related to the value of the linear charge density ξ by the following relations:

$$\begin{cases} \theta_{fix} = 1 - \dfrac{\xi_c}{\xi} \Longleftrightarrow \xi > \xi_c \\ \theta_{fix} = 0 \Longleftrightarrow \xi < \xi_c \end{cases} \tag{9}$$

where ξ_c is Manning's parameter critical value (i.e., the equilibrium value of linear charge density) that can be related to the valence of the counter-ions and of the fixed charges through the following equation:

$$\xi_c = \frac{1}{|z_c z_{fix}|} \tag{10}$$

where z_c is the counter-ion valence. Equations (9) and (10) are the mathematical expressions of Manning's limiting law, according to which, at infinite dilution, the equilibrium condition represents a singularity, characterised by the specific threshold value ξ_c, that only depends on the charge number of the counter-ions. Equation (9) implies that if $\xi < \xi_c$ counter-ions condensation does not occur [8,12]. However, when applied to a multi-ionic system, the previous definition of ξ_c would determine an apparent paradox, because different equilibrium states would exist for counter-ions of different valence. This fact was clarified by Manning [22], who highlighted that, at infinite dilution and in the presence of mixed-valence counter-ions, only the counter-ions at the highest valence should condense until the equilibrium value for condensation (ξ_c) is reached. This would suggest that the actual ξ_c may be determined by considering the maximum counter-ions valence. Another inherent limitation of the limiting law is that it does not provide a way to evaluate the condensed fraction of each counter-ion, as equations (9) and (10) alone are insufficient to determine the entire set of condensed fractions. A feasible approach is suggested by Manning's general theory, according to which the condensed fractions of counter-ions can be related by a mass-action-like law:

$$\frac{\frac{\theta_i}{1-\theta_i}}{\frac{\theta_j}{1-\theta_j}} = a_{i,j} \tag{11}$$

where $a_{i,j}$ assumes the meaning of a condensation selectivity. Despite being an elusive quantity to determine, the condensation selectivity may be related to the counter-ions condensation free energy, corresponding to the difference in counter-ions' free energy between the condensed and the uncondensed state [22]. Particularly, the counter-ions in the condensed state are likely to be at least partially dehydrated, as the region near the polyelectrolyte chains, where condensed counter-ions are localized, is presumably characterized by a lower dielectric constant. Assuming that the condensation free energy corresponds to the energy required for the partial dehydration of the counter-ions, the difference in condensation free energy between two distinct counter-ions can be related to their Born radii, in accordance with the Born model [23,24]. Consequently, the following equation can be used to estimate the condensation selectivity:

Table 1
Hydration numbers [26], *Crystal radii* [27], *Born radii* [23] *and Hydration free energy* [26] *of the ionic species considered in this study.*

	Hydration Number	Crystal radius [Å]	Born radius [Å]	ΔG^{hyd} [kJ mol^{-1}]
Na^+	3.5	0.95	1.68	−365
K^+	2.6	1.33	2.17	−295
Mg^{2+}	10.0	0.65	1.46	−1,830
Ca^{2+}	7.2	0.99	1.86	−1,505
Cl^-	2.0	1.21	3.32	−340

$$a_{i,j} = \frac{r_i}{r_j}\frac{z_j^2}{z_i^2} \tag{12}$$

where r_i and r_j are respectively the Born radii of the *i*-th and *j*-th species. According to the previous selectivity rule, inspired by the Born approximation, counter-ions with higher Born radius exhibit higher condensation selectivity and, thus, would be preferentially absorbed inside the membrane. As can be inferred from Table 1, the Born radius of an ionic species can be correlated to its crystal radius and its hydration number. Experimental tests performed by several authors confirmed that IEMs would select species with a higher crystal radius, characterised by a lower hydration number, as their partial dehydration would be thermodynamically favoured compared to species with smaller crystal radius [15,17,25]. As discussed in the following sections, equation (12) allowed to effectively describe the condensed counter-ions distribution in a multi-ionic system without any adjustable parameters.

2.4. Extended Donnan - peNRTL model

While the Manning model has been extensively used to predict ion activity coefficients in the membrane, its applicability was investigated mainly within a range of external concentrations between 0.01 and 1.0 *mol* l^{-1}. Beyond this range, several authors have reported a reduction in the predictive model capability [5,13]. This might be attributed to the potential breakdown of the model's underlying assumptions, including the condition of infinite dilution, which, according to Manning, should be consistent only up to a salt concentration of 0.1 *mol* l^{-1}. Furthermore, a significant limitation of the Manning model is its exclusive consideration of the long-range electrostatic interactions between the absorbed mobile ions and the polyelectrolyte chains. This simplification could be valid in a dilute system where the ion-chain interactions are dominant but may be misleading at high salt concentrations when other interactions, such as the electrostatic interactions between the mobile ions and the short-range (i.e., Van der Waals-like) interactions, could significantly influence the system. These types of interaction are generally accounted for in advanced thermodynamic models for aqueous electrolytes, such as the Pitzer model [20], in order to enlarge the concentration range of applicability. A modified Manning's activity coefficient, based on the application of the Pitzer model, was already proposed by Wells in 1973 to account for the mutual interactions between the mobile ions in a polyelectrolyte solution [28]. A similar approach was recently followed by Chen et al. that, starting from the eNRTL model developed for salt solutions [21], proposed the peNRTL model as an improved framework to evaluate the activity coefficients of charged species in a mixed salt-polyelectrolyte solution [29]. Later, the peNRTL model was successfully applied to describe the salt sorption of a set of tailor-made IEMs equilibrated with simple NaCl solutions in a concentration range between 0.01 and 1.0 *mol* l^{-1} [19]. The model is based on the assumption that different non-ideal phenomena additively contribute to the excess free energy of the system. Accordingly, the activity coefficients in the membrane could be evaluated as a combination of different contributions arising from different types of non-ideal interactions:

$$ln\left(\gamma_i^{(m),m}\right) = ln\left(\gamma_i^{(m),PDH}\right) + ln\left(\gamma_i^{(m),LC}\right) + ln\left(\gamma_i^{(m),M}\right) \tag{13}$$

where $\gamma_i^{(m),PDH}$ and $\gamma_i^{(m),LC}$ are respectively the contribution to the activity coefficient given by the point-to-point (i.e., ion-ion) long-range electrostatic interactions and the local contribution given by the short-range interactions, which together constitute the so-called eNRTL model. If $\gamma_i^{(m),M}$ is evaluated through the multi-ionic version of the model developed in section 2.3, equation (13) can be used to predict the ions' activity coefficients in the membrane for a multi-ionic system. The point-to-point electrostatic interaction term in equation (13) is evaluated through the Pitzer-Debye-Hückel (PDH) model; a simplified version of the Pitzer model for aqueous solution [30]:

$$ln\left(\gamma_i^{(x),PDH}\right) = -A_\varphi\left[\left(\frac{2z_i^2}{\rho}\right)ln\left[1+\rho I_x^{1/2}\right] + \frac{z_i^2 I_x^{1/2} - 2I_x^{3/2}}{1+\rho I_x^{1/2}}\right] \tag{14}$$

In the previous equation, A_φ and ρ are respectively the Debye-Hückel constant and the closest approach parameter [30], while I_x is the molar fraction-based ionic strength:

$$I_x = \frac{1}{2}\sum_i z_i^2(1-\theta_i)x_i^m \tag{15}$$

$$\frac{1}{z_c}\gamma_c^{(x),LC} = \frac{X_w G_{cw}}{\sum_i X_i G_{iw}}\left(\tau_{cw} - \frac{\sum_i X_i G_{iw}\tau_{iw}}{\sum_i X_i G_{iw}}\right) + \frac{\sum_{i\neq c} X_i G_{ic}\tau_{ic}}{\sum_{i\neq c} X_i G_{ic}} + \sum_a \frac{X_a G_{ca}}{\sum_{i\neq a} X_i G_{ia}}\left(\tau_{ca} - \frac{\sum_{i\neq a} X_i G_{ia}\tau_{ia}}{\sum_{i\neq a} X_i G_{ia}}\right) - \left(G_{cw}\tau_{cw} + \tau_{wc}\right) \tag{16}$$

where x_i^m is the molar fraction of the *i-th* ionic species in the membrane, which can be easily related to the molal concentrations in the membrane (equation (S8) in Supporting Material). Note that in equation (15), the sum includes the molar fraction of the fixed charges, while θ_i values are included to account for the condensed species. The superscript (x) in equation (14) denotes that the activity coefficients are evaluated on a molar-fraction scale. The molar fraction-based activity coefficients can be straightforwardly converted to the molal-based activity coefficients by applying equation (S9) provided in Supporting Material. It is worth noting that the PDH equation provides the same activity coefficient for species with the same charge number, as the only ion-specific property in equation (14) is the valence. The short-range interactions contribution is calculated through a local composition model, developed specifically for systems containing charged species, inspired by the nonrandom two-liquids model of Renon and Prausnitz [31]. The final equations used to evaluate the local contribution to the activity coefficients for the ionic species are provided below:

$$\frac{1}{z_a}\gamma_a^{(x),LC} = \frac{X_w G_{aw}}{\sum_i X_i G_{iw}}\left(\tau_{aw} - \frac{\sum_i X_i G_{iw}\tau_{iw}}{\sum_i X_i G_{iw}}\right) + \frac{\sum_{i\neq a} X_i G_{ia}\tau_{ia}}{\sum_{i\neq a} X_i G_{ia}} + \sum_c \frac{X_c G_{ac}}{\sum_{i\neq c} X_i G_{ic}}\left(\tau_{ac} - \frac{\sum_{i\neq c} X_i G_{ic}\tau_{ic}}{\sum_{i\neq c} X_i G_{ic}}\right) - (G_{aw}\tau_{aw} + \tau_{wa}) \quad (17)$$

$$G_{ij} = exp\left(-\alpha_{ij}\tau_{ij}\right) \quad (18)$$

$$X_i = |z_i| x_i^m \quad (19)$$

In the previous equations, X_i is the effective molar fraction of species i, the subscripts c, a and w denote respectively cationic species, anionic species and water. α_{ij} and τ_{ij} are respectively the nonrandomness factor (equal to 0.2 [19]) and the non-adjustable asymmetric binary interaction parameters between species i and j, which are used to describe the short-range interactions. In evaluating the sum, it should be pointed out that $i \neq c$ or $i \neq a$ means that all the cationic species and the anionic species, respectively, are excluded from the operation, while the binary parameters τ_{ii} involving the same species are 0 by definition. Furthermore, in equation (19) the charge number of the solvent $|z_i|$ is considered one [21]. Further discussion related to the evaluation of the binary interaction parameters, required to apply equations (16) and (17), is reported in section 2.6.

2.5. Model implementation

The models presented in section 2 were implemented on MatLab® to perform ion partitioning simulations. Their key characteristics are briefly summarized in Table 2.

Each ion partition model solves the Donnan equilibria (equation (1) or (5)) at the solution-membrane interface, to evaluate the equilibrium concentration of the ions within the membrane. The ideal Donnan model is the simplest of the three; however, it does not take into account the non-ideal phenomena neither in the external solution nor in the membrane. In contrast, both the Donnan–Manning model and the Donnan–peNRTL model account for these factors. The activity coefficients in the external solution are evaluated through the eNRTL model, while the activity coefficients in the membrane are evaluated through either the Manning model or the peNRTL model. As the activity coefficients in the membrane phase are related to the equilibrium concentration of the ions, the mathematical system of equations requires iterative solving. The initial guess for the equilibrium concentrations is provided by the ideal Donnan model. A schematic representation of the solving algorithm is reported in Fig. 1.

2.6. Manning's model parameters estimation

In order to apply the Manning model, a certain number of parameters must be known. Specifically, the linear charge density ξ of the chosen membrane must be determined. According to equation (6), at a fixed ambient temperature, ξ only depends on the relative dielectric constant of the hydrated membrane and on the fixed charges distance on the polymeric chains. Several authors have previously suggested that the relative dielectric constant of the wet membrane can be evaluated as a weighted average between the dielectric constant of the water and the dry polymer, in accordance with the following equation [8]:

$$\varepsilon_r = \varphi_w \varepsilon_w + (1 - \varphi_w)\varepsilon_p \quad (20)$$

where ε_w and ε_p are respectively the relative dielectric constant of pure water and of the dry polymer, while φ_w is the water volume fraction in the membrane. Assuming volumes additivity, φ_w can be easily related to the water uptake according to the following relation [13]:

$$\varphi_w = \frac{w_u}{w_u + \frac{\rho_w}{\rho_p}} \quad (21)$$

where ρ_w is the density of water at ambient temperature while ρ_p is the density of the dry polymer. In this work, all the above-mentioned membrane-related properties were experimentally evaluated, except for ε_p for which an average value of 6 was chosen. This choice is supported by the observation of Kamcev et al. who demonstrated that, within the range of values of ε_p for commercial IEMs (between 2 and 10), Manning's activity coefficient does not significantly depend on the value of dry polymer dielectric constant [13,14]. Regarding the value of b, some authors tried to correlate the average distance between the fixed charges to the membrane chemical structure and IEC [14,32]. However, this approach yielded poor predictions in some cases, even when the membrane's chemical structure was well-known [19]. This is probably related to the rather complex structure of the membranes that makes the theoretical evaluation of the average fixed charges distance a complex task to accomplish. When the actual value of b can be evaluated neither theoretically nor experimentally, ξ can be treated as an adjustable parameter. This approach allows for the semi-predictive application of Manning's model under various operative conditions since the linear

Table 2
Comparison of tested ion partition models. n represents the number of counter-ions in the system.

		Ideal Donnan	Donnan - Manning	Donnan - peNRTL
Accounted non-ideal phenomena	Ext. Solution non-ideality	✗	✓	✓
	Ion-Chain interactions	✗	✓	✓
	Ion-Ion interactions	✗	✗	✓
	Short-range interactions	✗	✗	✓
	Calibration parameters	None	ξ	ξ, $\tau_{i,j}$, $\tau_{j,i}$
	N° of fitting parameters	0	1	$1 + 2n$
	Suggested concentration range	$m^s \gg m_{fix}$	$m^s \ll m_{fix}$	Any
	Model complexity	Simple	Relatively simple	Complex
	Main equations	(2), (5)	(1), (2), (7)	(1), (2), (7), (14), (18), (19)

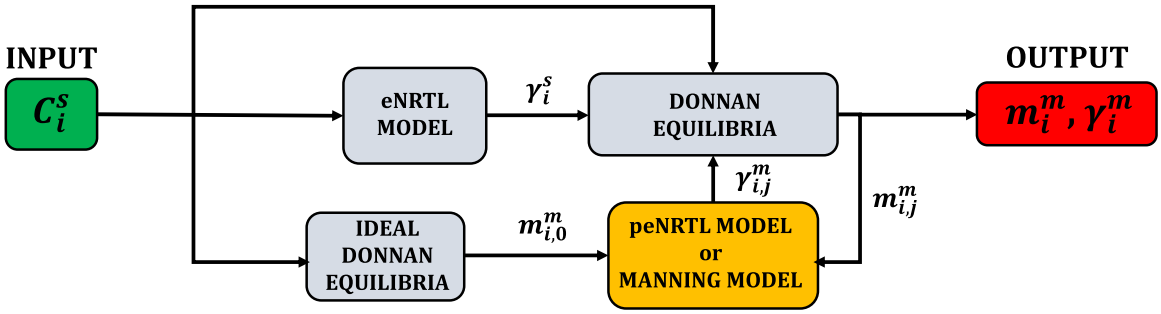

Fig. 1. Schematic representation of the Donnan-Manning and Donnan-peNRTL resolution algorithm implemented on MatLab®. Since the activity coefficients in the membrane depend on the ions' equilibrium concentration, a built-in non-linear solver was used to find the equilibrium concentration and the activity coefficients. The solver's initial guess is provided by the ideal Donnan model. The input molar concentrations in the solution are previously converted to molal concentrations through equation (S10) provided in Supplementary Material.

charge density is assumed to be independent of the external solution composition [17,33]. However, it is worth noting that, as the water uptake of the membrane can vary with the external concentration, according to equations (20) and (21), ξ is not strictly constant. Therefore, in this work b was treated as an adjustable parameter to account for potential changes in ξ due to variations in the membrane water content. Similarly to other works [29,33], the parameter was calibrated in order to minimize the Mean Relative Deviation (MRD) between the ion partitioning model predictions and the single-salt tests experimental data, which is hereafter defined:

$$MRD = \frac{1}{N}\sum_i \frac{\left|m_i^{m,exp.} - m_i^{m,pred.}\right|}{m_i^{m,exp.}} \tag{22}$$

In the definition of MRD, N is the number of experimental data points, $m_i^{m,exp.}$ is the experimental value of ion concentration in membrane, while $m_i^{m,pred.}$ is the predicted value.

2.7. eNRTL model parameters estimation

In order to apply equations (16) and (17) a certain number of non-adjustable interaction parameters τ_{ij} must be known. They can be evaluated through a simple mixing rule, reported in Supplementary Material (S4), if the corresponding adjustable interaction parameters are fitted from the experimental data. The number of parameters required to describe the local interactions depends on the number of molecular components and ionic species present in the system. However, the advantage of the local composition models is that, once the interaction parameters are derived from experimental data for all the required species, the same set of parameters can be applied to model any systems containing the same species, as they are assumed to be independent of the system composition. Therefore, the interaction parameters involving the solvent (i.e., the water) and the electrolytes considered in this work were retrieved from previous literature on the thermodynamic modelling of aqueous electrolytes [34]. The retrieved parameters for the salts considered in this work are listed in Table 3.

Consequently, the unknown parameters are those accounting for the short-range interactions between the mobile species and the fixed charges. Assuming the water to be the only molecular component in the system, the total number of required adjustable binary parameters is $2n$, where n is the number of different counter-ions. Further discussion on the number and nature of the adjustable parameters is reported in Supporting Material. The fitting procedure is similar to that presented in section 2.6: the parameters were obtained by applying the Donnan–peNRTL model and performing a multi-variable optimization to minimize the MRD with the experimental data of the single-salt tests, as expressed by equation (22). The optimization variables were the entire set of missing parameters, including the fixed charges distance b that was fitted separately for the Donnan–Manning model and the Donnan–peNRTL model. The fitting parameters are reported in Table 5 in section 4.1.

3. Experimental

In this section, the procedure adopted for the experimental determination of the equilibrium concentration in the membrane is presented.

3.1. Materials

Ion partitioning experimental data were collected for the cationic membrane Fumasep FKE-50 provided by Fumatech. This non-reinforced

Table 3
Retrieved eNRTL adjustable binary interaction parameters for water-electrolyte interactions [34].

i-j pair	water - (Na^+, Cl^-)	water - (K^+, Cl^-)	water - (Mg^{2+}, Cl^-)	water - (Ca^{2+}, Cl^-)	(Na^+, Cl^-) - (K^+, Cl^-)	(Mg^{2+}, Cl^-) - (Ca^{2+}, Cl^-)
τ_{ij}	8.865	8.170	10.854	10.478	0.386	0.332
τ_{ji}	−4.541	−4.153	−5.409	−5.291	−0.389	0.220

Table 4
Fumasep FKE-50 properties. The "measured" quantities are the averages of the experimental values obtained for each membrane sample. The fixed charges concentration, the water uptake and the IEC were determined following the procedure explained in section 3.5. The dry thickness was measured using a micrometre, while the dry density was determined as the ratio between the dry mass of the samples and their dry volume, evaluated as the product between the average thickness and the dry surface area. The reported values were taken from FuelCell store technical datasheet [35].

	m_{fix} [mol Kg_w^{-1}]	w_u [g_w g_{dry}^{-1}]	IEC [mmol g_{dry}^{-1}]	Dry Thickness [μm]	ρ_{dry} [g cm^{-3}]
Measured in this work	4.24 ± 0.4	0.35 ± 0.024	1.51 ± 0.04	54 ± 1.5	1.35 ± 0.03
Literature data [35]	7 ± 3	0.25 ± 0.1	1.45 ± 0.05	50 ± 5	1.6 ± 0.3

membrane is primarily used in water demineralization processes such as ED or CDI. The membrane was delivered in dry foils in the H^+ form. Its specifications, available in the literature, are detailed in Table 4. The chemicals used, including sodium chloride (NaCl ≥99%), potassium chloride (KCl, ≥99.5%), magnesium chloride ($MgCl_2$ > 99%), calcium chloride ($CaCl_2$, ≥96%) and nitric acid (HNO_3 ≥ 99.9%) were purchased from Carlo Erba Reagent (Italy). All the solutions were prepared using demineralized water $(\sigma < 1\ \mu S\ cm^{-1})$, which was obtained by treating tap water with a reverse osmosis unit and with a further purification step using ion-exchange resins.

3.2. Equilibration

The experimental procedure followed to determine the ions' equilibrium concentration in membrane is a well-established technique reported by several authors [5,17]. It is based on the equilibration of the membrane samples with a solution of chosen composition, followed by the desorption of the absorbed ionic species in a proper exchange solution. Membrane foils were cut into square samples of 64 cm^2. As received and prior to the equilibration step, the membrane samples were soaked in deionized water for 24 h to remove the residual fabrication solvent in the polymer matrix. The desorption water was changed once after 6 h. Subsequently, the samples were dipped in 50 g of the desired equilibrating solution for 24 h. The equilibrating solution was replaced once after 6 h to ensure perfect equilibration. The equilibrating time was chosen according to the procedure reported in the literature. Particularly, Galizia et al. reported that an equilibrating time below 24 h was enough to ensure perfect equilibration for all the investigated electrolytes [15]. The CEM samples were equilibrated with single-salt solutions of NaCl, KCl, $MgCl_2$, and $CaCl_2$ and binary equimolar mixtures of NaCl–KCl and $MgCl_2$–$CaCl_2$ in the range 0.1–5.0 $mol\ l^{-1}$ After the equilibration step, the samples were quickly washed by dipping into demineralized water to remove any excess salt on the surface, then blotted with tissue paper to remove excess water from the surface. The washing procedure is crucial for the outcome of the test, as it prevents the desorption solutions to be contaminated by the brine. To ensure that no mobile salt was lost during the washing, we carried out several preliminary tests to assess the impact of the rinsing procedure on the experimental outcomes, such as by varying the number of dips and the speed of dipping as well as the operator performing the rinsing. However, no significant correlation between these variables and the final experimental results was observed. After the washing step, wet samples were promptly weighed using an Ohaus Explorer EX324 analytical scale, avoiding weight loss due to spontaneous drying.

3.3. Co-ions sorption

In order to evaluate the amount of absorbed co-ions, subsequent to the equilibration procedure, the membrane samples were soaked with 50 g of deionized water to let the membrane desorb the co-ions in the form of mobile salt. During preliminary tests, the samples were left to desorb the mobile salt for 48 h and the desorption water was renewed once after 24 h. However, since negligible salt concentration was observed in the second desorption solution, subsequent tests assumed complete salt desorption within 24 h in a single desorption step. The desorption solutions were analyzed for anions and cations concentrations using Ion Cromatography (IC) (Metrohm 882 compact IC plus, Metrohm 930 compact IC flex).

3.4. Counter-ions sorption

Counter-ion concentrations in the membrane were measured using an exchange electrolyte. Following mobile salt desorption in deionized water, the membrane samples were dipped for 48 h in 50 g of solution containing 0.5 $mol\ l^{-1}$ nitric acid used as exchange electrolyte. Initially, a concentration of 0.1 $mol\ l^{-1}$ of nitric acid was used but due to the lower affinity of the H^+ in comparison to the divalent cations Mg^{2+} and Ca^{2+}, complete release of counter-ions was not achieved. Preliminary tests shown that two desorption steps were sufficient to release all absorbed counter-ions, as no counter-ions were detected in the third desorption solution. Therefore, the exchange solution was renewed once after 24 h and then analyzed with IC to evaluate the amount of desorbed counter-ions.

3.5. Water uptake and ions concentration assessment

After the counter-ions desorption step, the samples were dried in a static oven (Argolab, TCN50 Plus) at 40 °C for 24 h, and then quickly weighed to prevent any absorption of moisture from the air. Finally, the membrane water uptake was assessed through the following equation:

$$w_u = \frac{M_{wet} - M_{dry}}{M_{dry}} \tag{23}$$

where M_{wet} and M_{dry} are respectively the wet mass of the sample after the equilibration step and the dry mass of the sample. The water uptake was then employed to evaluate the molal concentration of the ions in the membrane according to the following equation:

$$m_i^m = \frac{\sum_j M_j^{ds} \omega_{i,j}^{ds}}{M_{w,i} w_u M_{dry}} \tag{24}$$

where $\omega_{i,j}^{ds}$ is the mass fraction of ionic species i in the j-th desorption solution of mass M_j^{ds}, obtained from the chromatographic analysis, while $M_{w,i}$ is the molar weight of the ionic species i. The sum is extended to all the desorption steps. The fixed charges molal concentration was consequently evaluated by applying the electroneutrality condition in the membrane (equation (2)). Finally, the membrane IEC was evaluated according to the following equation:

$$IEC = m_{fix} w_u \tag{25}$$

The membrane properties measured during the ion-sorption tests are reported in Table 4. Regarding the experimental evaluation of the activity coefficients in the membrane, it is not possible to obtain the activity coefficient of a single species. However, by combining equation (1) applied to the generic species i and j, it is possible to obtain an expression to evaluate a combination of their activity coefficients in the membrane:

$$\frac{\left(\gamma_i^m\right)^{1/z_i}}{\left(\gamma_j^m\right)^{1/z_j}} = \left(\frac{m_i^s}{m_i^m}\right)^{\frac{1}{z_i}} \left(\frac{m_j^m}{m_j^s}\right)^{\frac{1}{z_j}} \frac{\left(\gamma_i^s\right)^{\frac{1}{z_i}}}{\left(\gamma_j^s\right)^{\frac{1}{z_j}}} \tag{26}$$

If i and j represent a cation and an anion, respectively, the left-hand side of equation (26) is somehow comparable to the mean ionic activity coefficient of the electrolyte.

4. Results and discussion

This section is devoted to the discussion of the experimental and modelling results of ion partitioning in the investigated CEM. Firstly, results for the single salt systems are presented (section 4.1). Then, results for the multi-ionic solutions are reported.

4.1. Single-salt tests

Firstly, single-salt ion sorption tests were carried out. Following the procedure explained in section 3, the CEM was equilibrated with solutions of NaCl, KCl, $MgCl_2$, and $CaCl_2$ spanning concentrations from 0.1 to 5.0 $mol\ l^{-1}$ or up to the solubility of the salt. In certain cases, exposure to highly concentrated solution can cause mechanical embrittlement

Table 5
Fitted Manning parameters and peNRTL adjustable binary parameters. CG-stands for the negatively charged groups in the polymeric matrix. The two models were calibrated separately on single-salt tests experimental data. The average ξ was evaluated from b, considering the average water uptake.

Model	i-j pair	τ_{ij}	τ_{ji}	*b* [nm]	*Average ξ*
Donnan-Manning	–	–	–	9.630	0.228
Donnan-peNRTL	water - (Na^+, CG-)	−9.492	−3.189	0.135	16.05
	water - (K^+, CG-)	−8.211	−2.939		
	water - (Mg^{2+}, CG-)	−8.164	−2.766		
	water - (Ca^{2+}, CG-)	−7.945	−2.465		

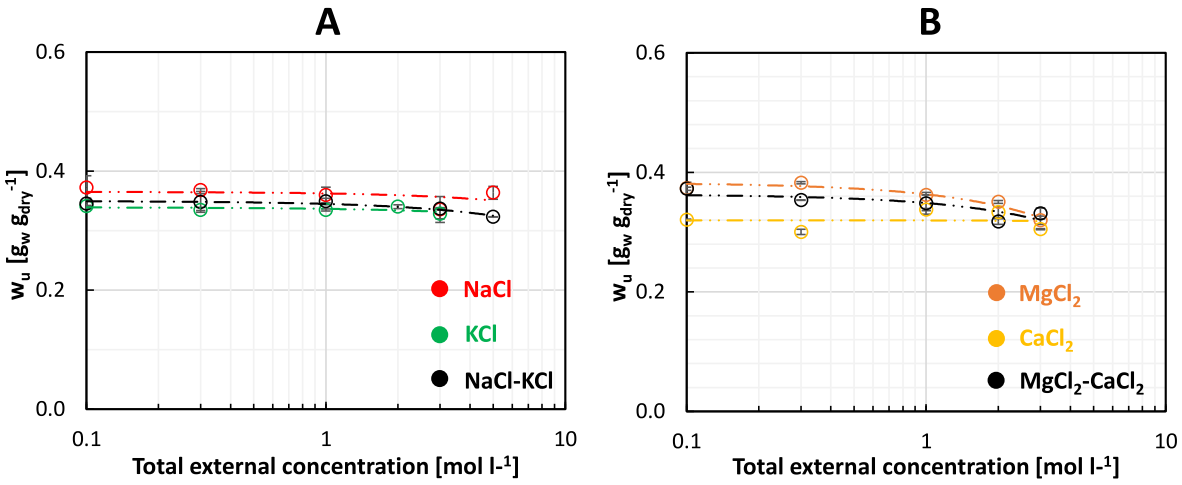

Fig. 2. Membrane water uptake versus the total external concentration for the single-salt and the binary mixtures tests. The empty circles are the experimental data, while the dash-dot lines are the linear regressions used to extrapolate the water-uptake trend as a function of the external concentration.

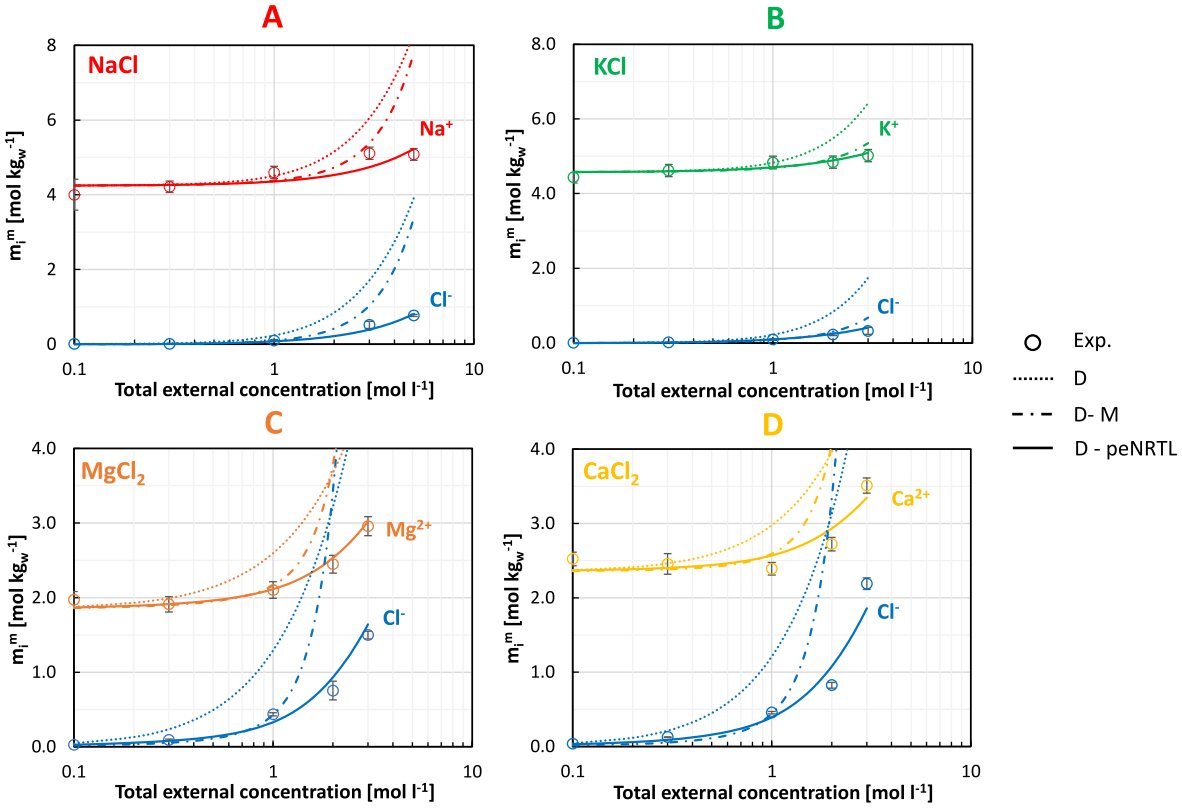

Fig. 3. Ions' molal concentration in membrane versus the external salt concentration for single salt systems containing NaCl (A), KCl (B), $MgCl_2$(C) or $CaCl_2$ (D). The empty circles are the experimental data. The associated error bars were plotted considering the maximum error between the theoretical error evaluated through the error propagation theory and the experimental error on at least two different tests. The dotted lines represent the predictions of the ideal Donnan model, the dash-dot lines represent the predictions of the Donnan-Manning model while the solid lines are the predictions of the Donnan–peNRTL model.

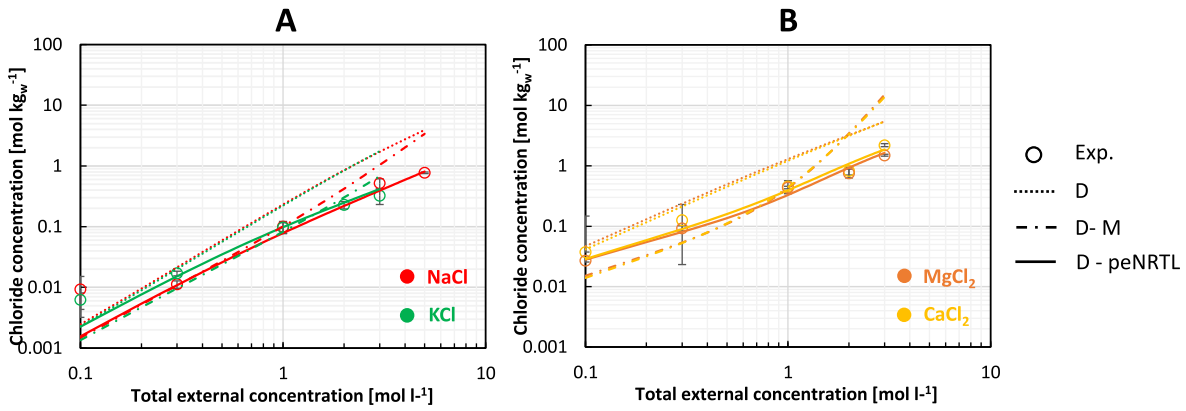

Fig. 4. Log-log plot of the co-ions molal concentration in membrane versus the external salt concentration for the single-salt systems containing NaCl or KCl (A), $MgCl_2$ or $CaCl_2$ (B). The empty circles are the experimental data. The associated error bars were plotted considering the maximum error between the theoretical error evaluated through the error propagation theory and the experimental error on at least two different tests. The dotted lines represent the predictions of the ideal Donnan model, the dash-dot lines represent the predictions of the Donnan-Manning model while the solid lines are the predictions of the Donnan–peNRTL model.

and cracks on the membrane surface due to the strongly osmotic deswelling. This point was not investigated in the present paper given that only blank samples were used to perform the tests. However, in the past, we had employed IEMs with very concentrated solutions many times and for many tests, even lasting for days, without observing any worsening in their performance. The investigated set of electrolytes was chosen such that the chloride was the only shared co-ion. As a result, any differences in the experimental results can be attributed to the nature of the counter-ions. Regarding the tests with $MgCl_2$ and $CaCl_2$ performed at external concentrations higher than 3.0 $mol\ l^{-1}$, the analysis of the exchange solutions found a negligible salt concentration. Apparently, when equilibrated with highly concentrated solutions containing Mg^{2+} or Ca^{2+}, the membrane was not able to release the absorbed ions, although the reason for this is not clear. Scaling phenomena associated with neutral salt precipitation inside the membrane matrix are likely to occur when the IEM is equilibrated with highly concentrated solutions containing $MgCl_2$, and $CaCl_2$, which are known to be scaling agents. Therefore, the tests involving the divalent species were performed at external concentrations up to 3.0 $mol\ l^{-1}$. The membrane water uptake versus the external solution concentration and composition is reported in Fig. 2.

For the investigated membrane, the water uptake was almost

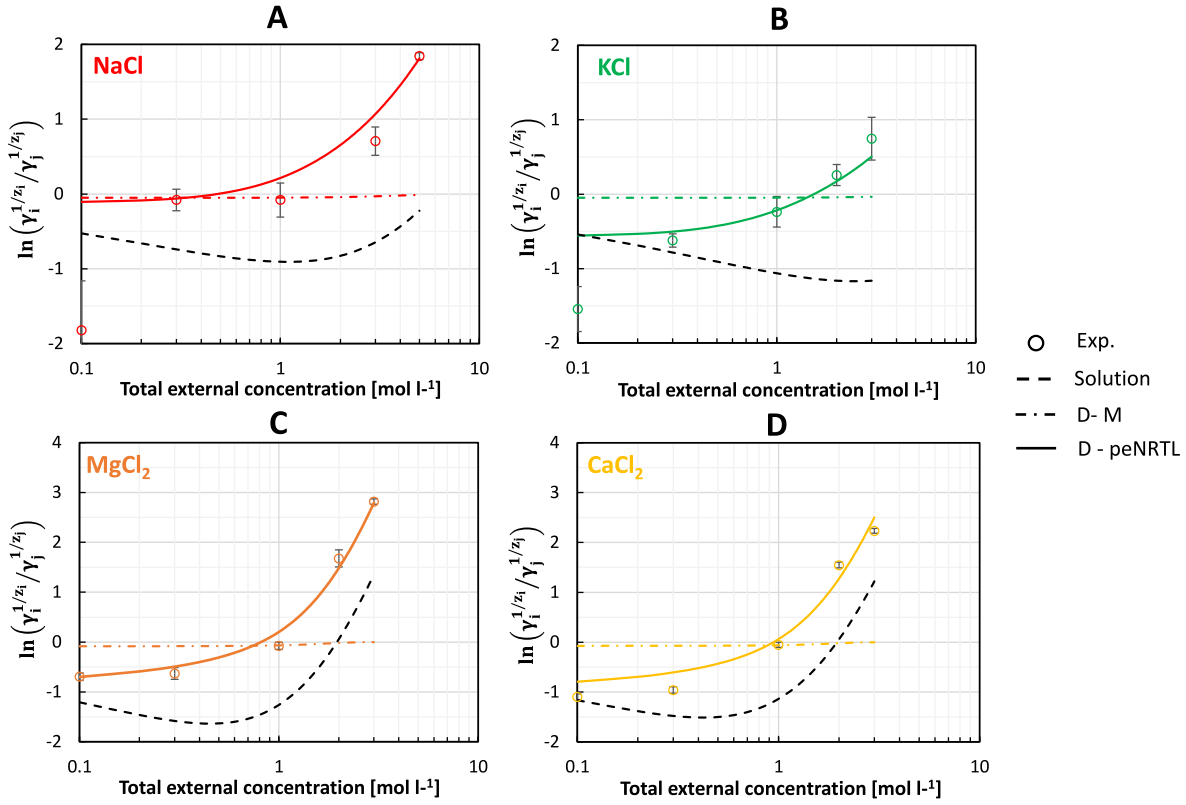

Fig. 5. Activity coefficients as a function of the external concentration for the single-salt systems containing NaCl (A), KCl (B), $MgCl_2$ (C) or $CaCl_2$ (D). The values on the Y axes were evaluated through equation (26) assuming that *i* refers to the counter-ion while *j* refers to the co-ion. The empty circles were obtained from experimental concentration in membrane, the dot-dash lines are the prediction of the Donnan–Manning model while the solid lines are the predictions of the Donnan-peNRTL model. The black dashed lines refer to the external solution activity coefficients and were obtained by applying the eNRTL model.

constant in the presence of monovalent cations, with a minor difference between NaCl and KCl. Contrastingly, there was a slight decrease in water uptake at high concentrations of $MgCl_2$ and $CaCl_2$. It is well known that the amount of water absorbed is related to the concentration and composition of the external solution [14–16]. Particularly at high external concentration, the sorption of mobile salt in the membrane phase is associated with an increase in the osmotic pressure difference between the solution and the membrane, thus reducing the water uptake of the membrane due to a phenomenon called osmotic deswelling [36]. Generally, the water uptake can significantly influence ion sorption. Indeed, according to equation (25), the amount of absorbed water is inversely related to the fixed charges concentration, which determines to a large extent the amount of absorbed co-ions. The experimental equilibrium concentrations of co-ions and counter-ions in the membrane phase are shown in Fig. 3.

The sorption of the co- and counter-ions exhibit similarities for the pairs NaCl, KCl and $MgCl_2$, $CaCl_2$. Notably, the equilibrium concentration of Mg^{2+} or Ca^{2+} in the membrane phase is approximately half that of Na^+ and K^+, due to their divalent charge. At low external concentration, the amount of absorbed co-ions (shown in Figs. 3 and 4) is negligible due to the Donnan exclusion effect, and, consequently, the counter-ion concentration approaches the fixed charge concentration.

Conversely, at high external salt concentration, the concentration of the co-ions increases due to the weakening of the Donnan exclusion effect, which is correlated to a reduction in the Donnan potential. As depicted in Fig. 4, the co-ion concentration increases almost linearly in a log-log scale with the external salt concentration. The increase in co-ion sorption is particularly pronounced for the divalent cations Mg^{2+} and Ca^{2+} because the Donnan potential is inversely related to the valence of the counter-ions. Therefore, at a fixed external salt concentration, the presence of divalent cations results in a higher co-ion concentration [17]. The co-ion concentration in the membrane phase is also directly related to the absorbed mobile-salt concentration, as equivalent numbers of counter-ions and co-ions are absorbed to maintain electroneutrality in the membrane. In Figs. 3 and 4, the experimental equilibrium concentrations in the membrane phase are directly compared to the results of the ion partition simulations. The ideal Donnan model was directly applied, while the Donnan-Manning model and the Donnan–peNRTL model were calibrated separately, according to the procedure reported in section 2.6. The fitting parameters are reported in Table 5. The values of ξ reported in Table 5 were calculated from equation (6), considering an average value for the relative dielectric constant. Given that the value of b could not be experimentally determined, the models were intentionally calibrated separately in order to compare them to the best of their predictive capabilities. The two values of b minimize the MRD of the two models, respectively. Consequently, we can assert that any other values would provide worse results.

Interestingly, the average value of ξ that minimizes the error of the Donnan–Manning model is below the condensation threshold value, while the value of ξ fitted with the Donnan–peNRTL model is well above ξ_c. Consequently, according to the Manning limiting law (equation (9)), counter-ions are assumed to be partially condensed by the Donnan–peNRTL model and totally uncondensed by the Donnan–Manning model. These discrepant results could be due to the limited range of applicability of the limiting law from which the actual ξ value was inferred. When considering an ion-exchange membrane, the presence of fixed charges prevents the condition of infinite dilution (i.e., $\kappa b \ll 1$ [22]) from being satisfied, especially when the IEM is equilibrated with highly concentrated solutions [37]. Nonetheless, its direct application remains appealing owing to its mathematical simplicity. Therefore, when dealing with highly concentrated solutions, ξ should be considered as a mere fitting constant without purporting it to have a specific physical meaning.

From the direct comparison among the proposed models in Figs. 3 and 4, it is evident that the Donnan-peNRTL model outperforms the others at high external concentrations. This can be easily explained by considering the values of the electrolyte activity coefficients reported in Fig. 5.

Table 6
Mean relative error of the investigated ion partition model. The reported values are calculated by applying equation (22) and accounting for the experimental error bars associated with the measurements.

Test	Ideal Donnan	Donnan-Manning	Donnan - peNRTL
NaCl	82.5%	50.0%	6.6%
KCl	72.3%	19.1%	5.1%
NaCl–KCl	56.2%	39.7%	6.2%
$MgCl_2$	102.0%	149.3%	3.5%
$CaCl_2$	73.3%	111.8%	10.6%
$MgCl_2$–$CaCl_2$	83.9%	148.2%	5.7%
Average	78.4%	86.4%	6.3%

At external salt concentrations higher than 1.0 $mol\,l^{-1}$, the electrolyte activity coefficient in the membrane becomes higher than 1 for all the investigated electrolytes. According to equation (7), the Manning model can not predict an activity coefficient in the membrane higher than 1. In fact, the derivative of the excess free energy of interaction between the mobile ions and the fixed charge, expressed in equation (S4), is always negative. This is consistent with the fact that an increase in the ionic strength causes a reduction of the Debye length of the system and, hence, an increase in the electrostatic interactions that tend to stabilize the system. Moreover, the counter-ion condensation further reduces the activity coefficients. Therefore, the fitting procedure results in a value of ξ below the condensation threshold value in order to minimize the MRD at high external concentrations. It is worth noting that in the majority of the works reported in the literature, the Donnan-Manning model was applied semi-predictively, calibrating ξ on ion partitioning data up to a total external concentration of 1.0 $mol\,l^{-1}$, for which the activity coefficients in the membrane were systematically lower than 1. This may be correlated to the fact that the majority of the ξ values reported in the literature for different membrane types are higher than the condensation threshold values of monovalent and divalent counter-ions. As previously discussed, the assumptions of the Manning model are expected to break down at high external concentrations. Moreover, this model only takes into account the electrostatic interactions between the mobile ions and the linear charge distribution on the polymeric chains, thus neglecting any other interactions that could play a key role at high external concentrations. Fig. 5 demonstrates that the failure of the Donnan-Manning model at high external concentrations is related to an increase in the activity coefficients in the solution, which is not offset by a corresponding increase of the Manning activity coefficients in the membrane. According to equation (1), this fact leads the model to overestimate the salt concentration in the membrane (see Fig. 3). The same problem was encountered by Galizia et al., who applied the Donnan-Manning model to predict $CaCl_2$ sorption at an external concentration exceeding 1.0 $mol\,l^{-1}$ [5]. To address this issue, they introduced an empirical correction term to the membrane activity coefficient evaluated through the Pitzer model [20]. The latter is capable of predicting activity coefficients in solution higher than 1, taking into account the short-range interactions between the ionic species, which are dominant at high concentrations because of the reduced distance between the ionic species. The same is likely to occur in the membrane phase. In particular, when the absorbed salt concentration becomes comparable to the fixed charge concentration, the short-range interactions are expected to outweigh the ion-chain interactions, which would no longer be dominant. A summary of the comparison between the three ion partition models is presented in Table 6, where MRD values of each model applied to the different cases investigated are reported.

The average MRD for the Donnan–peNRTL model is nearly 6.3%, which is far lower than the MRD of the comparison models. Interestingly, the MRD of the divalent counter-ion tests is lower for the ideal Donnan model than for the Donnan–Manning model. A similar result

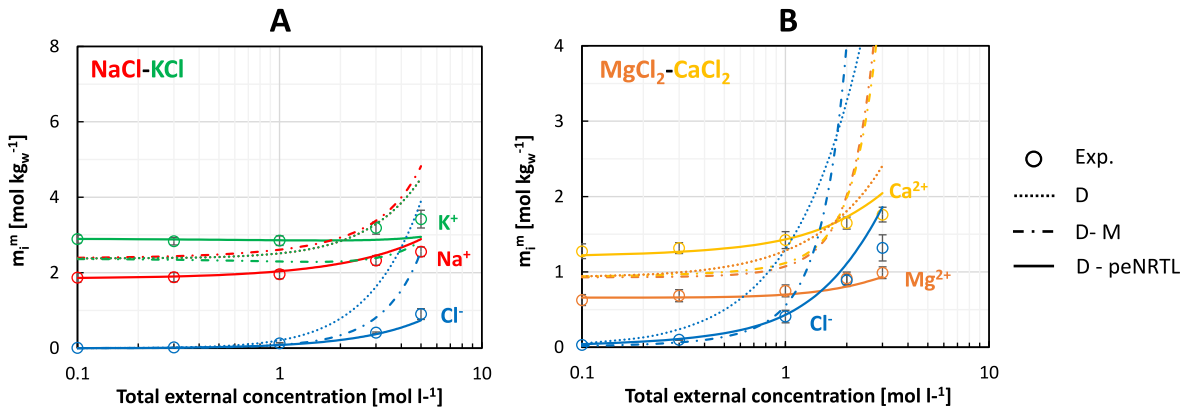

Fig. 6. Co- and counter-ions equilibrium molal concentrations versus total external salt concentration for the two equimolar mixtures of NaCl–KCl (A) and $MgCl_2$–$CaCl_2$ (B). The empty circles are the experimental data. The associated error bars were plotted considering the maximum error between the theoretical error evaluated through the error propagation theory and the experimental error on at least two different tests. The dotted lines represent the predictions of the ideal Donnan model, the dash-dot lines represent the predictions of the Donnan-Manning model while the solid lines are the predictions of the extended Donnan–peNRTL model.

was obtained in high-concentration tests carried out by Galizia et al. [5]. This observation is consistent with the hypothesis that, at high mobile salt concentrations in the membrane, the ion-chain interactions are no longer dominant. Therefore, at infinite concentration, the activity coefficients in the membrane would ideally approach those in the solutions, thus validating the basic assumption of the ideal Donnan model. Consequently, the ideal Donnan model could be successfully applied whenever the external salt concentration is far higher than the fixed charges concentration in the membrane. In the Donnan–Manning model instead, the activity coefficients in the membrane are evaluated by taking into account only the ion-chain interactions. Consequently, the model provides good predictions when the main contribution to the activity coefficients stems from the interactions between the mobile ions and the linear charge distribution, i.e., when the mobile salt concentration is negligible compared to the fixed charges concentration. By contrast, in the Donnan–peNRTL model, the short-range interactions are captured by the local contribution of the nonrandom two-liquid model, which provides an increase in the membrane activity coefficients at high external concentration, improving the prediction of the mobile salt sorption at high external concentration.

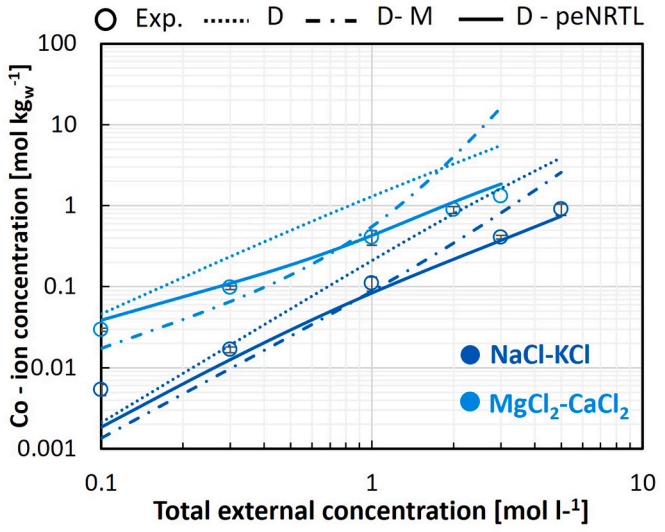

Fig. 7. Log-log plot of co-ions equilibrium concentration in membrane for the binary mixture tests versus the total external salt concentration. The empty circles are the experimental data corresponding to the chloride concentration reported in Fig. 6 A and B. The associated error bars were plotted considering the maximum error between the theoretical error evaluated through the error propagation theory and the experimental error on at least two different tests. The dotted lines represent the predictions of the idea Donnan model, the dash-dot lines represent the predictions of the Donnan-Manning model while the solid lines are the predictions of the extended Donnan–peNRTL model.

4.2. *Binary mixtures tests*

Ion partitioning tests with binary equimolar mixtures of NaCl–KCl and $MgCl_2$–$CaCl_2$ in the range of 0.1–5.0 $mol\,l^{-1}$ were carried out in order to validate the extended Donnan-peNRTL model for predicting the ion partition in multi-ionic systems. The binary solutions were prepared using electrolytes containing cations with similar valence to highlight the influence of the ions' inherent nature on the counter-ion distribution in the membrane. The experimental equilibrium concentrations in the membrane are reported in Fig. 6.

In the NaCl–KCl system, the counter-ions' concentration remained almost constant up to an external concentration of 1.0 $mol\,l^{-1}$. Beyond this concentration, an increase in co-ion sorption caused a rise in counter-ions' concentration. The slight decrease in water uptake, shown in Fig. 2, may also be related to an increase in the ion concentrations in the membrane, given that the concentrations are reported on a water mass basis. The experimentally observed partition selectivity S_{K^+/N_a^+} was approximately 1.4 and was relatively constant over the entire range of concentration, being not significantly influenced by the total external concentration. The higher partition selectivity of K^+ over Na^+ has been previously documented in the literature [10,17] and is allegedly due to the different hydration states of the two cations. Particularly, the sorption in membrane would be more favourable for the ion with the larger crystal radius. According to the Born model of ion solvation in fact, the transfer of an ion to an environment with a lower dielectric constant would be thermodynamically more favourable for ions with a larger Born radius [38]. Similar findings apply to the tests involving divalent cations. The $S_{C_a^{2+}/M_g^{2+}}$ sorption selectivity was about 1.9, and it was relatively independent of the external concentration as well. This outcome was expected, given that Ca^{2+} has a crystal radius larger than Mg^{2+}. Furthermore, the trend in co-ions concentration (depicted in Fig. 7) for the two mixtures closely resembled the co-ions sorption trend observed in the single-salt tests with counter-ions of equal valence, suggesting that the presence of two different counter-ions with the same valence does not significantly affect the co-ion sorption.

The ion partition experimental data are compared with the predictions of the proposed models in Fig. 6. The simulations were performed using the same set of parameters reported in Table 5 that were

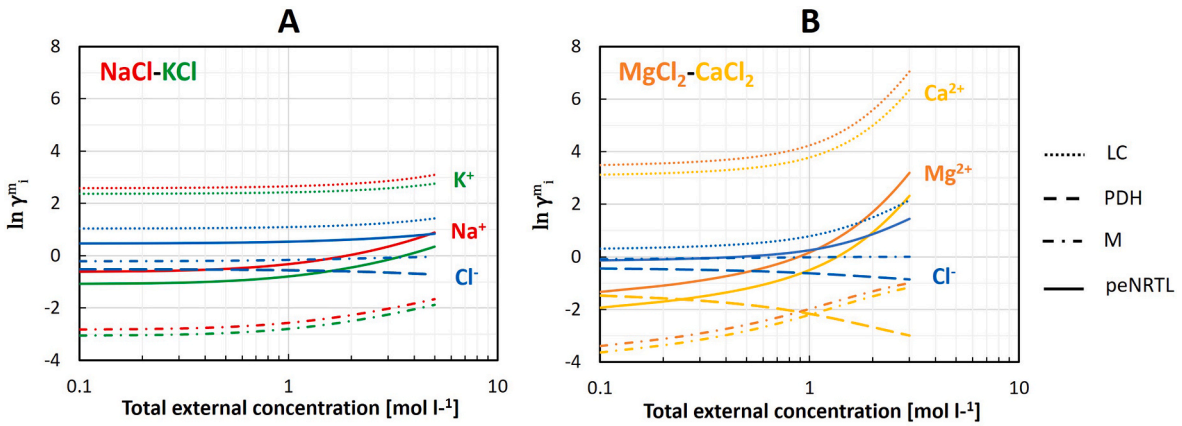

Fig. 8. Ions activity coefficients in membrane versus the external total salt concentration, for the binary systems NaCl–KCl (A) and $MgCl_2$–$CaCl_2$ (B). The solid lines are the activity coefficients estimated through the extended peNRTL model (eq. (13), the dotted lines are the local contribution to the activity coefficients (equation (16) and (17) and the dashed lines represent the PDH contribution (equation (14)) and the dash-dot lines are the Manning contribution (equation (7)).

fitted on the single-salt tests. Both the ideal Donnan model and the extended Donnan-Manning model tend to overestimate the concentration of co-ions in the membrane, particularly at total external concentrations exceeding 1.0 $mol\,l^{-1}$, especially for the $MgCl_2$–$CaCl_2$ system. This is primarily because, as discussed earlier, both models fail to account for the increased activity coefficients in the membrane occurring at high external concentrations. Moreover, both the ideal Donnan model and the extended Donnan-Manning model fail to accurately describe the partition selectivity of counter-ions. Notably, according to equation (5), the ideal Donnan model predicts equal partitioning coefficients of counter-ions with the same valence. Regarding the extended Donnan-Manning model, its failure in predicting the counter-ions partition can be explained by considering that the value of ξ obtained from the calibration is lower than the critical condensation values of each of the counter-ions. Consequently, the condensation selectivity rule presented in equation (12) is not taken into account by the model, as the counter-ion condensation is not occurring. The difference in the equilibrium concentrations of Na^+ and K^+, or Mg^{2+} and Ca^{2+} are then solely related to the difference in their activity coefficients in the solution. As can be inferred from Fig. 5, Mg^{2+} and Ca^{2+} have similar activity coefficients in the external solution. Consequently, the Donnan-Manning model lines for these two ions are almost overlapped in Fig. 6B. In contrast, the extended Donnan-peNRTL model successfully quantifies both co-ions and counter-ions partition across the entire range of external concentrations examined. For both the NaCl–KCl and $MgCl_2$–$CaCl_2$ mixtures, the counter-ion partition selectivity is well-captured thanks to the proposed condensation selectivity rule (equation (12)) for the extended Manning model. To the best of the authors' knowledge, this is the first time that the counter-ions' distribution between an IEM and a multi-ionic solution is quantitatively predicted without adjustable parameters up these extremely high external concentrations. The combination of the three contributions of the peNRTL model for the evaluation of the activity coefficients was fundamental in extending the validity range of the model. As depicted in Fig. 8, for both NaCl–KCl (A) and $MgCl_2$–$CaCl_2$ (B) systems, the extended peNRTL model predicts an increase in the activity coefficients in the membrane, thereby preventing the sharp rise in the concentration of mobile ions predicted by the ideal Donnan and Donnan-Manning models. This increase can be rationalized by analyzing separately the three contributions, which are reported in Fig. 8.

The PDH contribution is always negative and decreasing at high concentration, according to the fact that the long-range electrostatic interactions are stronger for low values of the Debye length. Notably, the PDH contributions in Fig. 8 (A and B) are overlapped because the PDH model does not differentiate between ions with the same charge number, as indicated in equation (14). The Manning model contribution is also negative, as discussed in section 4.1, but unlike the PDH, it increases with the external concentration. This increase can be addressed to the condensation phenomenon. In fact, while the fraction of condensed fixed charges is independent of the external concentration, the amount of absorbed counter-ions increases to counterbalance the charge of the absorbed co-ions. This results in a reduced fraction of condensed counter-ions, leading to an increase in the Manning activity coefficient. Conversely, the local contributions are always positive, implying that the short-range interactions are of a repulsive nature. Moreover, the local contribution is increasing with the external concentration, following a trend similar to the co-ions concentration. At high concentrations, short-range interactions typically increase due to the decreased distance between species. This explains why the local contributions in the $MgCl_2$–$CaCl_2$ system are higher and increase more rapidly compared to the NaCl–KCl system. For a similar reason, at low external concentration, when the co-ions concentration in the membrane approaches 0, both the local contribution and the PDH contributions are almost constant, as the counter-ions concentration approaches a constant value. Noticeably, the absolute values of the local and PDH contributions to the co-ion activity coefficient are almost equal. Therefore, the two terms tend to cancel out each other and consequently, at low external concentrations, the Manning model provides the most relevant contribution to the activity coefficient This observation suggests that at external concentrations below 1.0 $mol\,l^{-1}$, the partitioning of co-ions is dominated by ion-chain interactions.

5. Conclusions

In this work, we developed a novel ion partitioning model for IEMs equilibrated with multi-ionic solutions. Manning's counter-ions condensation model was extended to account for the presence of different ionic species. Moreover, a condensation selectivity rule based on the Born approximation for the dehydration free energy of the counter-ion was proposed to evaluate the condensed fractions for different counter-ions without adjustable parameters. Despite the hydration number of the counter-ions can vary significantly when they are absorbed into the membrane, the proposed condensation selectivity rule was applied successfully as the counter-ions charge density, and thus their Born radii, remain almost unchanged. The extended version of the Manning model was merged with the peNRTL to broaden the applicability range of the two models. Novel ion sorption tests were performed to validate the proposed model, with four different single-salt solutions and two different binary equimolar mixtures, using the commercial CEM Fumasep FKE-50. The tests performed with binary mixtures of counter-ions with similar valence pointed out the importance of the hydration state of the counter-ions in determining the partition selectivity. The cationic membrane exhibited a higher affinity towards the species with

the larger crystal radii and hence with the lower charge density. The concentrations of K^+ and Ca^{2+} in the membrane were higher than the concentrations of Na^+ and Mg^{2+}, respectively. Moreover, the K^+/Na^+ and Ca^{2+}/Mg^{2+} partition selectivity remained largely unaffected by the total external concentration. Co-ions sorption in the binary mixture tests was similar to the single-salt tests performed with salt containing cations of the same valence, suggesting that the presence of two different counter-ions with the same charge has minimal impact on mobile salt sorption. Finally, the ideal Donnan model, the extended Donnan-Manning model and the extended Donnan-peNRTL model were compared to assess the predictive capacity of the proposed model. The models were used to semi-empirically predict the ion partitioning in the single-salt systems. The extended Donnan-Manning model failed in the prediction of the ion sorption equilibria at concentrations higher than 1.0 $mol\,l^{-1}$, while the extended Donnan-peNRTL model here proposed was able to quantitively predict the ion concentrations in membrane over the entire concentration range investigated. This suggests that the interactions neglected by the Manning model would play a key role at high external concentrations. With the same set of fitting parameters, the extended Donnan–peNRTL was able to quantitively describe the ion sorption equilibria also for the investigated binary systems, proving that the set of the eNRTL binary parameters is independent of the composition. The proposed condensation selectivity rule allowed us to predict the partitioning in membrane of different counter-ions, requiring no additional adjustable parameters. In conclusion, we can assert that the hydration state of the counter-ions should be taken into account to predict the counter-ions partition in membrane. Furthermore, accounting for different types of interaction, such as short-range interactions, is crucial in order to extend the range of applicability of the ion partition models. Further study will be carried out to test the predictive capability of the extended Donnan-peNRTL model in more complex multi-ionic systems, including species with different valence, thus investigating the specific effect of the Donnan potential on the sorption selectivity.

CRediT authorship contribution statement

Giorgio Purpura: Writing – original draft, Validation, Software, Methodology, Investigation, Formal analysis, Data curation, Conceptualization. **Ewa Papiewska:** Investigation. **Andrea Culcasi:** Writing – review & editing, Supervision, Software, Methodology, Conceptualization. **Antonia Filingeri:** Supervision, Investigation, Writing – review & editing. **Alessandro Tamburini:** Writing – review & editing, Validation, Supervision, Resources, Project administration, Methodology, Funding acquisition, Data curation, Conceptualization. **Maria Chiara Ferrari:** Supervision. **Giorgio Micale:** Writing – review & editing, Supervision, Resources, Project administration. **Andrea Cipollina:** Writing – review & editing, Supervision, Resources, Project administration, Methodology.

Declaration of competing interest

The authors declare that they have no known competing financial interests or personal relationships that could have appeared to influence the work reported in this paper.

Data availability

Data will be made available on request.

Acknowledgements

This work was supported by the EU within SEArcularMINE (Circular Processing of Seawater Brines from Saltworks for Recovery of Valuable Raw Materials) project − Horizon 2020 programme, Grant Agreement no. 869467. This output reflects only the author's view. The European Health and Digital Executive Agency (HaDEA) and the European Commission cannot be held responsible for any use that may be made of the information contained therein.

Appendix A. Supplementary data

Supplementary data to this article can be found online at https://doi.org/10.1016/j.memsci.2024.122659.

Nomenclature

A_φ	*Debye-Hückel constant [−]*
a	*Condensation selectivity [−]*
b	*Average distance between fixed charges [m]*
C	*Molar concentration [mol* m^{-3}*]*
e	*Elementary charge [C]*
F	*Faraday constant [C* mol^{-1}*]*
IEC	*Ion-Exchange Capacity [mol* $kg^{-1}_{dry\ polymer}$*]*
I_x	*Molar fraction-based Ionic strength [−]*
K	*Partitioning coefficient [−]*
k_B	*Boltzman's constant [J* K^{-1}*]*
M	*Mass [kg]*
MW	*Molar mass [kg* mol^{-1}*]*
m	*Molal concentration [mol* kg^{-1}*]*
N	*Number of data points [−]*
N_a	*Avogadro's number [*mol^{-1}*]*
n	*Number of moles [mol]*
R	Universal gas constant [J mol^{-1} K^{-1}]
r	*Ion Born radius [m]*
S	*Sorption selectivity [−]*
T	*Temperature [K]*
v	Partial molar volume [m^3 mol^{-1}]
w_u	Water uptake [kg_{water} $kg^{-1}_{dry\ polymer}$]
X	*Effective molar fraction [−]*
x	*Molar fraction [−]*

z	*Ion valence [−]*

Greek symbols

α	*Nonrandomness parameters [−]*
γ	*Activity coefficient [−]*
ε_0	*Vacuum dielectric constant [F m^{-1}]*
ε_w	*Water relative dielectric constant [−]*
ε_p	*Dry polymer relative dielectric constant [−]*
ε_r	*Wet membrane average relative dielectric constant [−]*
θ	*Counter-ion condensed fraction [−]*
κ	*Debye screening parameters [m^{-1}]*
λ_b	*Bjerrum length [m]*
ξ	*Reduced linear charge density [−]*
ξ_c	*Reduced critical linear charge density [−]*
φ	*Electrostatic potential [V]*
$\Delta\varphi$	*Donnan potential [V]*
ρ	*Closest approach parameter [−]*
τ	*Binary asymmetric interaction parameters [−]*
φ_w	*Swelling degree [−]*
ω	*Mass fraction [−]*

Superscript/ Subscript

(m)	*Molal-based*
(x)	*Molar fraction-based*
s	*Solution phase*
m	*Membrane phase*
0	*Standard state*
M	*Manning contribution*
PDH	*Pitzer-Debye-Hückel contribution*
LC	*Local contribution*
ds	*Desorption solution*
$exp.$	*Experimental point*
$pred.$	*Predicted point*
i,j	*Component*
fix	*Fixed charges*
w	*Water*
c	*Cationic species*
a	*Anionic species*
wet	*Wet membrane*
dry	*Dry membrane*
p	*Ion containing polymer*

Acronyms

CDI	Capacitive De-ionization
ED	Electrodialysis
EDBM	Electrodialysis with bipolar membrane
MCD	Membrane Capacitive Deionization
IEM	Ion-Exchange Membrane
AEM	*Anion-Exchange Membrane*
CEM	*Cation-Exchange Membrane*
MRD	*Mean Relative Deviation*

References

[1] A. Campione, L. Gurreri, M. Ciofalo, G. Micale, A. Tamburini, A. Cipollina, Electrodialysis for water desalination: a critical assessment of recent developments on process fundamentals, models and applications, Desalination 434 (2018) 121–160, https://doi.org/10.1016/j.desal.2017.12.044.

[2] A. Culcasi, L. Gurreri, A. Cipollina, A. Tamburini, G. Micale, A comprehensive multi-scale model for bipolar membrane electrodialysis (BMED), Chem. Eng. J. 437 (2022) 135317, https://doi.org/10.1016/j.cej.2022.135317.

[3] A. Campione, A. Cipollina, E. Toet, L. Gurreri, I.D.L. Bogle, G. Micale, Water desalination by capacitive electrodialysis: Experiments and modelling, Desalination 473 (2020) 114150, https://doi.org/10.1016/j.desal.2019.114150.

[4] J. Kamcev, M. Galizia, F.M. Benedetti, E.S. Jang, D.R. Paul, B.D. Freeman, G. S. Manning, Partitioning of mobile ions between ion exchange polymers and aqueous salt solutions: importance of counter-ion condensation, Phys. Chem. Chem. Phys. 18 (2016) 6021–6031, https://doi.org/10.1039/c5cp06747b.

[5] M. Galizia, G.S. Manning, D.R. Paul, B.D. Freeman, Ion partitioning between brines and ion exchange polymers, Polymer (Guildf) 165 (2019) 91–100, https://doi.org/10.1016/j.polymer.2019.01.026.

[6] J.C. Díaz, J. Kamcev, Ionic conductivity of ion-exchange membranes: measurement techniques and salt concentration dependence, J. Memb. Sci. 618 (2021) 118718, https://doi.org/10.1016/j.memsci.2020.118718.

[7] J. Kamcev, D.R. Paul, G.S. Manning, B.D. Freeman, Ion diffusion coefficients in ion exchange membranes: significance of counterion condensation, Macromolecules 51 (2018) 5519–5529, https://doi.org/10.1021/acs.macromol.8b00645.

[8] D. Kitto, J. Kamcev, Manning condensation in ion exchange membranes: a review on ion partitioning and diffusion models, J. Polym. Sci. 60 (2022) 2929–2973, https://doi.org/10.1002/pol.20210810.

[9] H.M. Saif, R.M. Huertas, S. Pawlowski, J.G. Crespo, S. Velizarov, Development of highly selective composite polymeric membranes for Li+/Mg2+ separation,

J. Memb. Sci. 620 (2021) 118891, https://doi.org/10.1016/j.memsci.2020.118891.
[10] S. Ozkul, J.J. van Daal, N.J.M. Kuipers, R.J.M. Bisselink, H. Bruning, J.E. Dykstra, H.H.M. Rijnaarts, Transport mechanisms in electrodialysis: the effect on selective ion transport in multi-ionic solutions, J. Memb. Sci. 665 (2023) 121114, https://doi.org/10.1016/j.memsci.2022.121114.
[11] H. Strathmann, Ion-Exchange Membrane Separation Processes, First, Elsevier B.V., 2004.
[12] G.S. Manning, Limiting laws and counterion condensation in polyelectrolyte solutions I. Colligative properties, J. Chem. Phys. 51 (1969) 924–933, https://doi.org/10.1063/1.1672157.
[13] J. Kamcev, D.R. Paul, B.D. Freeman, Ion activity coefficients in ion exchange polymers: applicability of Manning's counterion condensation theory, Macromolecules 48 (2015) 8011–8024, https://doi.org/10.1021/acs.macromol.5b01654.
[14] E.-S.S. Jang, J. Kamcev, K. Kobayashi, N. Yan, R. Sujanani, S.J. Talley, R.B. Moore, D.R. Paul, B.D. Freeman, Effect of water content on sodium chloride sorption in cross-linked cation exchange membranes, Macromolecules 52 (2019) 2569–2579, https://doi.org/10.1021/acs.macromol.8b02550.
[15] M. Galizia, F.M. Benedetti, D.R. Paul, B.D. Freeman, Monovalent and divalent ion sorption in a cation exchange membrane based on cross-linked poly (p-styrene sulfonate-co-divinylbenzene), J. Memb. Sci. 535 (2017) 132–142, https://doi.org/10.1016/j.memsci.2017.04.007.
[16] N. Yan, D.R. Paul, B.D. Freeman, Water and ion sorption in a series of cross-linked AMPS/PEGDA hydrogel membranes, Polymer (Guildf) 146 (2018) 196–208, https://doi.org/10.1016/j.polymer.2018.05.021.
[17] G.Q. Chen, K. Wei, A. Hassanvand, B.D. Freeman, S.E. Kentish, Single and binary ion sorption equilibria of monovalent and divalent ions in commercial ion exchange membranes, Water Res. 175 (2020) 115681, https://doi.org/10.1016/j.watres.2020.115681.
[18] R. Wang, R. Duddu, S. Lin, Extended Donnan-Manning theory for selective ion partition and transport in ion exchange membrane, J. Memb. Sci. 681 (2023) 121782, https://doi.org/10.1016/j.memsci.2023.121782.
[19] Y. Yu, N. Yan, B.D. Freeman, C.-C.C. Chen, Mobile ion partitioning in ion exchange membranes immersed in saline solutions, J. Memb. Sci. 620 (2021) 118760, https://doi.org/10.1016/j.memsci.2020.118760.
[20] K.S. Pitzer, J.J. Kim, Thermodynamics of electrolytes. IV activity and osmotic coefficients for mixed electrolytes, J. Solution Chem. 3 (1974) 539–546, https://doi.org/10.1007/BF00648138.
[21] Y. Song, C.C. Chen, Symmetric electrolyte nonrandom two-liquid activity coefficient model, Ind. Eng. Chem. Res. 48 (2009) 7788–7797, https://doi.org/10.1021/ie9004578.
[22] G.S. Manning, Limiting laws and counterion condensation in polyelectrolyte solutions. 8. Mixtures of counterions, species selectivity, and valence selectivity, J. Phys. Chem. 88 (1984) 6654–6661, https://doi.org/10.1021/j150670a030.
[23] A.A. Rashin, B. Honig, Reevaluation of the Born model of ion hydration, J. Phys. Chem. 89 (1985) 5588–5593, https://doi.org/10.1021/j100272a006.
[24] K. Chang, H. Luo, G.M. Geise, Influence of salt concentration on hydrated polymer relative permittivity and state of water properties, Macromolecules 54 (2021) 637–646, https://doi.org/10.1021/acs.macromol.0c02188.
[25] T. Luo, S. Abdu, M. Wessling, Selectivity of ion exchange membranes: a review, J. Memb. Sci. 555 (2018) 429–454, https://doi.org/10.1016/j.memsci.2018.03.051.
[26] Y. Marcus, Thermodynamics of Solvation of Ions 87 (1991) 2995–2999, https://doi.org/10.1039/FT9918702995.
[27] E.R. Nightingale, Phenomenological theory of ion solvation. Effective radii of hydrated ions, J. Phys. Chem. 63 (1959) 1381–1387, https://doi.org/10.1021/j150579a011.
[28] J.D. Wells, Thermodynamics of polyelectrolyte solutions, Biopolymers 12 (1973) 223–227.
[29] Y. Yu, Y. Li, N. Hossain, C.C. Chen, Nonrandom two-liquid activity coefficient model for aqueous polyelectrolyte solutions, Fluid Phase Equilib 497 (2019) 1–9, https://doi.org/10.1016/j.fluid.2019.05.009.
[30] K.S. Pitzer, J.M. Simonson, Thermodynamics of multicomponent, miscible, ionic systems: theory and equations, J. Phys. Chem. 90 (1986) 3005–3009, https://doi.org/10.1021/j100404a042.
[31] H. Renon, J.M. Prausnitz, Local compositions in thermodynamic excess functions for liquid mixtures, AIChE J. 14 (1968) 135–144, https://doi.org/10.1002/aic.690140124.
[32] T. Luo, Y. Zhong, D. Xu, X. Wang, M. Wessling, Combining Manning's theory and the ionic conductivity experimental approach to characterize selectivity of cation exchange membranes, J. Memb. Sci. 629 (2021) 119263, https://doi.org/10.1016/j.memsci.2021.119263.
[33] R.S. Kingsbury, S. Zhu, S. Flotron, O. Coronell, Microstructure determines water and salt permeation in commercial ion-exchange membranes, ACS Appl. Mater. Interfaces 10 (2018) 39745–39756, https://doi.org/10.1021/acsami.8b14494.
[34] S. Tanveer, C.C. Chen, A comprehensive thermodynamic model for high salinity produced waters, AIChE J. 66 (2020) 3–7, https://doi.org/10.1002/aic.16818.
[35] FKE-50 Techincal Specification, 2008, p. 282. https://www.fuelcellstore.com/spec-sheets/fumasep-fke-50-technical-specifications.pdf.
[36] P.J. Flory, J. Rehner, Statistical mechanics of cross-linked polymer networks II, Swelling, J. Chem. Phys. 11 (1943) 521–526, https://doi.org/10.1063/1.1723792.
[37] S. Paoletti, J. Benegas, A. Cesàro, G. Manzini, F. Fogolari, V. Crescenzi, Limiting-laws of polyelectrolyte solutions. Ionic distribution in mixed-valency counterions systems. I: the model, Biophys. Chem. 41 (1991) 73–80, https://doi.org/10.1016/0301-4622(91)87211-M.
[38] J.R. Bontha, P.N. Pintauro, Water orientation and ion solvation effects during multicomponent salt partitioning in a Nafion cation exchange membrane, Chem. Eng. Sci. 49 (1994) 3835–3851, https://doi.org/10.1016/0009-2509(94)00205-3.